Review

Recent Progress on Layered Double Hydroxides for Electrocatalytic Small Molecules Oxidation to Synthesize High-Value Chemicals and Degrade Pollutants

Zi-Qi Ge [1] Chao Chu [2] Cong Wang [3] Ruchun Li [4,*] Jingwei Li [2,*] San Ping Jiang [2,*]

[1] Jilin Joint Technology Innovation Laboratory of Developing and Utilizing Materials of Reducing Pollution and Carbon Emissions, College of Engineering, Jilin Normal University, Siping 136000, China
[2] National Energy Key Laboratory for New Hydrogen-Ammonia Energy Technologies, Foshan Xianhu Laboratory, Foshan 528216, China
[3] Bingtuan Energy Development Institute, Shihezi University, Shihezi 832000, China
[4] Faculty of Chemistry and Chemical Engineering, Yunnan Normal University, Kunming 650500, China
***** Correspondence: S.Jiang@curtin.edu.au (S. P. J.); lijingwei@xhlab.cn (J. L.); liruchun@ynnu.edu.cn (R. L.)
Received: 25 October 2025; Revised: 12 November 2024; Accepted: 6 December 2024; Published: 10 December 2024

Abstract: Replacing the high thermodynamic potential oxygen evolution reaction with the fast and low energy barrier electrocatalytic small molecule oxidation reaction (ESMOR), coupling of the hydrogen evolution reaction, has shown the promising potential to reduce the energy consumption of electrolyzers. Layered double hydroxides (LDHs), with their adjustable properties further improved by doping, heterojunction construction, and morphology optimization, have emerged as highly promising catalysts for ESMOR. This review summarizes the recent advancements in LDH-based catalysts for the ESMOR, including alcohols, aldehydes, hydrazine, urea, and sulfide ions. This review also outlines the principles and advantages of coupling small molecule oxidation with water splitting for producing high-value chemicals and degrading pollutants. The current challenges in catalyst design, investigation of reaction mechanisms, and product separation are further highlighted. Finally, the review discusses the challenges and future prospects of LDH-based catalysts for small molecule oxidation reactions, with the aim of stimulating further research and advancement in electrocatalytic oxidation technologies.

Keywords: layered double hydroxides; electrocatalytic small molecules oxidation reaction; oxygen evolution reaction; hydrogen evolution reaction; high-value chemicals; pollutant degradation

1. Introduction

Hydrogen is a potential alternative energy source to fossil fuels due to its high energy density (120 MJ/kg) and green emissions [1,2]. However, as hydrogen does not exist in accessible quantities in nature, green hydrogen is best produced from the water electrolysis technology powered by renewable electricity [3,4]. In this process, the anodic oxygen evolution reaction (OER) involves a four-electron process, which is kinetically slow and has high energy consumption [5,6]. The anodic electrocatalytic small molecule oxidation reaction or ESMOR in short, such as alcohols, aldehydes, hydrazine, and urea have lower thermodynamic overpotentials and are widely considered as the ideal alternatives to the OER [7,8]. However, the ESMOR still faces key challenges, including inefficient catalyst performance and poor stability.

Two-dimensional materials are excellent candidates for developing efficient catalysts due to their larger specific surface area, highly exposed coordination unsaturated sites, and unique electronic properties [9–11]. Layered Double Hydroxides (LDHs) are a typical two-dimensional material consisting of cation-exchange layers between two layers of hydroxide (Figure 1) [12,13]. The general formula of LDHs can be summarized as $[M_{1-x}^{2+}M_x^{3+}(OH)_2]^{x+}(A^{n-})_{x/n}\cdot mH_2O$, composed of cation-exchange layers between two hydroxide layers. The divalent metal ions M_{1-x}^{2+} are typically Ni^{2+}, Co^{2+}, Mg^{2+}, etc., and trivalent metal ions M^{3+} are usually Fe^{3+}, Al^{3+}, Cr^{2+}, etc. The anions A^{n-} are often OH^-, CO_3^{2-}, NO_3^-, and other inorganic and organic ions. Depending on the interlayer anion, the interlayer spacing is different, forming a hexagonal network structure [14–16]. These metal layers in LDHs are intercalated with hydroxide ions or other anions to maintain electrical neutrality [16]. In addition, by introducing other metal atoms into the LDHs layers, it can be transformed into ternary LDHs or multi-metal LDHs, which can generate more active sites and adjust the electronic structure, thereby further tuning the

catalytic activity [17–20]. Even synergistic effects between multiple metal centers can control the catalytic reaction through interactions or changes in the surrounding electronic structure [21–23]. In summary, the excellent electronic structure, abundant active sites and high tunability of LDHs make them a promising 2D material for electrocatalysis [24–26]. Moreover, researchers have also attempted to adjust the introduction of other elements by altering synthesis methods and routes in order to purposefully achieve structural regulation of multi-metal LDHs, with the goal of enhancing catalytic performance, which has consequently attracted increasing attention [27–29].

This review overviews the fundamental principles and current research status of LDHs in electrocatalytic small-molecule oxidation, including electrocatalytic oxidation of alcohols and aldehydes to synthesize value-added chemicals, as well as and electrocatalytic degradation of pollutants such as hydrazine hydrate and urea. The applicability of LDHs electrocatalysts for small-molecule anodic oxidation based on the current state of research, which provides a valuable guideline for exploring efficient yet promising catalysts for LDH-related materials were also summarized. In addition, we present perspectives on the applications of LDHs and their derivatives in electrocatalytic water splitting, oxidation of organic compounds to produce value-added chemicals, and degradation of pollutants.

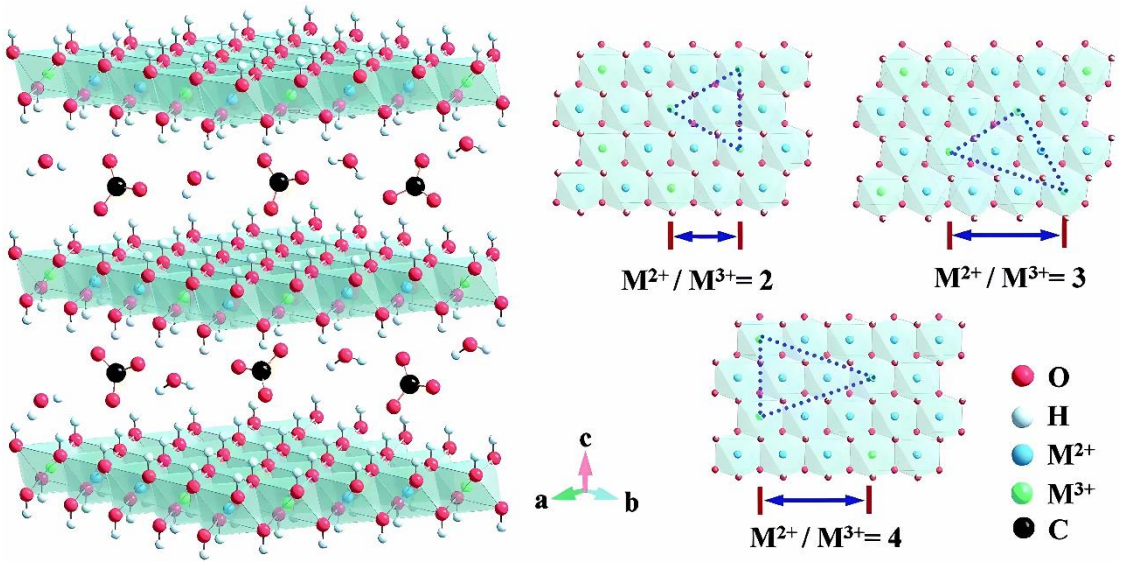

Figure 1. The crystal structure of LDHs.

2. Discovery and Development History of LDH

In 1842, Swedish scientists first discovered the natural LDH mineral—hydrotalcite, marking the starting point of the scientific community's formal recognition of LDHs materials. One hundred years late, Feitknecht and others first synthesized LDHs materials artificially by reacting metal salt solutions with alkali metal hydroxides and proposed the concept of the layered structure of LDHs (Figure 2a). In 1969, Allmann and Taylor successfully determined the single-crystal structure of LDHs using single-crystal X-ray diffraction, experimentally confirming the layered structure of LDHs for the first time. This discovery provided a crucial basis for the structural characterization and performance studies of LDHs [13].

In the 1970s, as research on LDHs materials advanced, scientists gradually discovered the anion exchange properties of LDHs. This finding revealed the initial application potential of LDHs materials in fields such as adsorption and catalysis. In the 1980s, researchers conducted in-depth studies on the products of annealed LDHs and successfully applied them in redox catalytic processes, further expanding the application areas of LDHs materials (Figure 2a) [30].

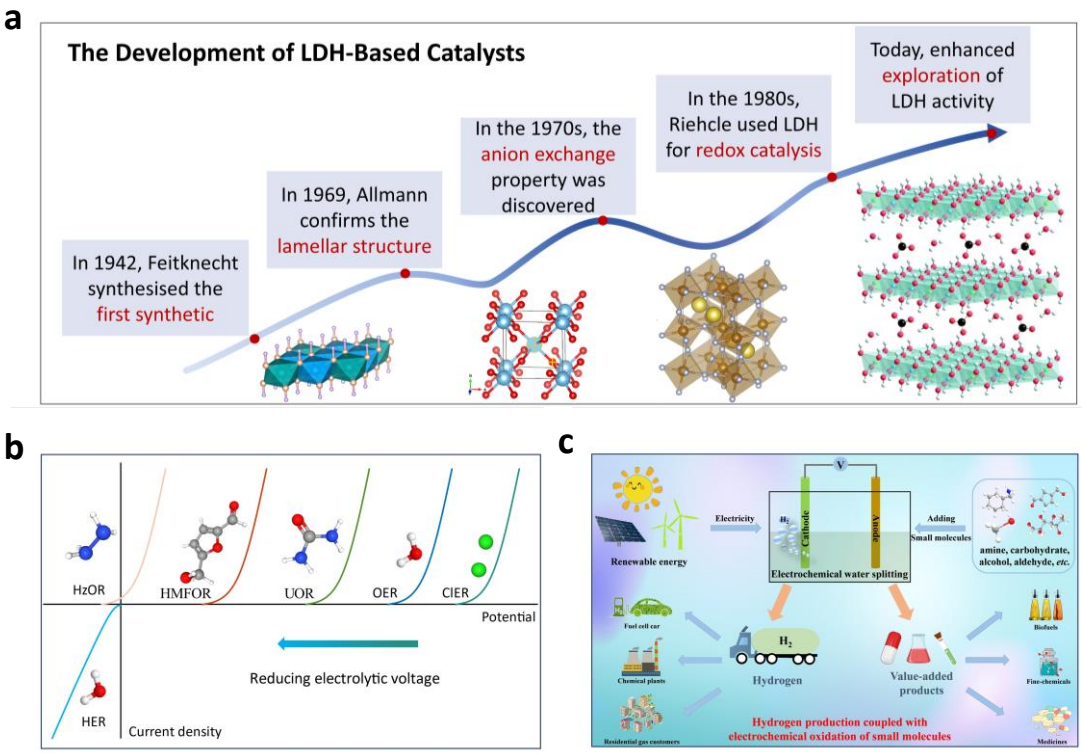

Figure 2. (**a**) The scheme for the development of LDHs. (**b**) Comparison of voltages for OER, CER, HER and the small-molecule oxidation reactions including hydrazine (HzOR), 5-hydroxymethylfurfural (HMFOR), and urea (UOR). (**c**) The blueprint of hydrogen production coupled with the electrocatalytic small molecule oxidation. (**b**,**c**) Reprinted with permission from [46]. Copyright 2024 Wiley-VCH GmbH.

In recent years, LDHs have demonstrated broad application prospects in various fields, including catalysis, medicine, energy storage, and environmental management. For example, in the field of electrocatalysis, bimetallic LDHs materials such as NiFe-LDH have garnered significant attention due to their excellent catalytic activity and selectivity [31,32]. In the field of electrochemical energy storage, including batteries, supercapacitors, sensors and secondary batteries, LDHs materials have also exhibited outstanding performance [33].

With the continuous deepening of understanding regarding the structure and properties of LDH materials, along with ongoing innovations in synthesis techniques, the performance and application range of LDH materials are expected to be further enhanced and expanded.

3. Fundamentals and Advantages for Electrocatalytic Small Molecular Oxidation

Electrocatalytic water splitting has become an important method for hydrogen production. However, the entire water electrolysis process is significantly limited by the thermodynamics and kinetics of the OER. Thermodynamically, the Gibbs free energy change for the anode OER at standard conditions (298 K, 101.325 kPa) is $\Delta G = 237.1$ kJ mol^{-1}, which requires an electrical energy of 1.23 V [23]. In terms of kinetics, OER as a four-electron transfer process leads to slow reaction rates, especially for industrial production where large current densities are required. Therefore, actual electrolyzer requires a voltage significantly higher than 1.23 V [34]. Electrocatalytic water splitting for hydrogen production involves different reaction mechanisms at the cathode and anode under acidic and alkaline conditions. The acidic hydrogen evolution reaction (HER) at the cathode is a two-electron-proton process, as shown in Equation (1), while the anode oxygen evolution reaction (OER) involves a four-electron-proton process, as shown in Equation (2) [35].

Water splitting in acidic electrolyte

$$2H^+ + 2e^- \rightarrow H_2 \ (0 \text{ V vs. RHE}) \quad (1)$$

$$2H_2O \rightarrow 4H^+ + O_2 + 4e^- \ (1.23 \text{ V vs. RHE}) \quad (2)$$

Under alkaline conditions, the cathodic HER involves the absorption of two electrons by two water molecules, leading to their dissociation into hydrogen gas and two hydroxide ions, as shown in Equation (3) [36]. At the anode, the OER involves the loss of four electrons by four hydroxide ions, resulting in the formation of two water

molecules and one oxygen molecule, as shown in Equation (4) [37]. This reaction also involves a four-electron transfer.

Water splitting in alkaline electrolyte

$$2H_2O + 2e^- \rightarrow H_2 + 2OH^- \text{ (0 V vs. RHE)} \quad (3)$$

$$4HO^- \rightarrow 2H_2O + O_2 + 4e^- \text{ (1.23 V vs. RHE)} \quad (4)$$

Under both acidic and alkaline conditions, the anode OER is a four-electron process. Due to the slow kinetics of the anode OER, it often becomes the main limiting factor for the efficiency of water electrolysis for hydrogen production [38,39]. In contrast, OER limits the energy conversion efficiency during hydrogen production and also affects the stability of the proton exchange membrane water electrolyzer. Currently widely used noble metal catalysts such as Ru and Ir-based catalysts reduce their large-scale use due to their high price and insufficient crust content. Therefore, in order to reduce the high energy consumption, it is an effective strategy to use small molecule oxidation reactions, which are thermodynamically more applicable, to replace the OER process. In recent years, hydrazine oxidation reaction (HzOR), urea oxidation reaction (UOR), and sulfur ion oxidation reaction (SOR) have garnered widespread interest due to their lower theoretical oxidation potentials (Figure 2b) [40,41]. The theoretical oxidation potentials for HzOR, UOR, and SOR are −0.33 V, 0.37 V, and −0.48 V, respectively, which are significantly lower than that of OER [42−44]. It suggests that the HzOR, UOR, and SOR may be more efficient than the OER and can be used for hydrogen production. The anodic reaction can be obtained from the following equation:

$$N_2H_4 + 4OH^- \rightarrow N_2 + 4H_2O + 4e^- \text{ (−0.33 V vs. RHE)} \quad (5)$$

$$CO(NH_2)_2 + 6OH \rightarrow N_2 + CO_2 + 5H_2O + 6e^- \text{ (0.37 V vs. RHE)} \quad (6)$$

$$S^{2-} - 2e^- \rightarrow S \text{ (−0.48 V vs RHE)} \quad (7)$$

Under alkaline conditions, the hydrazine oxidation reaction (HzOR) provides an energy-efficient method for hydrogen production, while also providing additional benefits such as the degradation of N_2H_4-contaminated wastewater and the production of low-value by-products like water (H_2O) and nitrogen gas (N_2), without generating CO_2 greenhouse gases, as shown in Equation (5) [45]. Moreover, HzOR has a lower theoretical voltage of −0.33 V, higher power density, and faster electrocatalytic kinetics. Additionally, UOR technology not only converts urea-containing wastewater into gaseous products but can also generate energy through thoughtful design [46]. Although UOR is a six-electron transfer process, as shown in Equation (6), it has a theoretical potential of only 0.37 V, making it widely applicable in the field of electrochemistry [47,48]. The thermodynamic potential of SOR (−0.48 V) is also significantly lower than that of OER. Moreover, H_2S or S^{2-} are common pollutants in industrial exhaust gases and wastewater, posing risks to human health and the environment. Therefore, employing anode SOR can oxidize S^{2-} or H_2S into valuable elemental sulfur without the need for additional oxidants or complex separation processes, as shown in Equation (7) (Figure 2c) [48].

4. Proposed Strategy on LDH for Electrocatalytic Small Molecular Oxidation

4.1. Electrocatalytic Oxidation of Small Molecular to Value-Added Chemicals

Electrocatalytic alcohol and aldehyde oxidation are not only a viable anodic reaction, but it can also be coupled to hydrogen evolution reactions (HER) or other reductive fuel production reactions in electrochemical and photoelectrochemical cells [49]. These reactions can effectively lower the cell potential and enable the conversion of inexpensive industrial feedstocks or renewable biomass resources into valuable products [50,51]. Meanwhile, simpler alcohols and aldehydes are converted into more valuable chemicals such as formic acid and dimethylfurans. The formic acid is an important raw material for leather processing and is also widely used in the degradation of plastic monomers, dyes, and food additives. Furthermore, the oxidation of 5-hydroxymethylfurfural (HMF) yields 2,5-furandicarboxylic acid (FDCA), which is widely regarded as the most suitable substitute for petroleum-derived terephthalic acid. Therefore, the oxidation of alcohols and aldehydes to produce value-added products is a subject of extensive research.

Methanol Oxidation Reaction to Formic Acid: For the LDH anode methanol oxidation system, methanol as a small-chain alcohol with high hydrogen content, need the least number of electrons for complete oxidation. Additionally, effective understanding the methanol oxidation (MOR) process can lead to more efficient production of high-value products from biomass [52]. Methanol (at $350 per ton) has been long used as a feedstock to produce

higher-value formic acid (at $1300 per ton), which are important chemicals in rubber and pharmaceutical industries [53]. Many transition metal-based LDHs catalysts have exhibited activity for MOR and used as an alternative to the OER in electrolyzers, enabling the production of value-added products such as formic acid. Song et al [54]. Synthesized defect-rich ultra-thin u-NiV-LDH, which optimizes the electronic structure of Ni sites (Figure 3a–c). When applied to MOR, u-NiV-LDH exhibits a low potential of 1.41 V vs. RHE at 100 mA cm^{-2}, which is significantly lower than that of bulk NiV-LDH at the same current density (Figure 3d). After reaction for five cycles, the yields of H_2 and formic acid are 98.2% and 88.1%, respectively (Figure 3e,f). Sun et al [55]. demonstrated efficient and stable MOR in alkaline media by anchoring Pt nanoparticles onto the surface of NiFe-LDHs. In this system, the single-atom dispersed Fe^{3+} in the NiFe-LDH layers serves as anchoring sites for Pt precursors, ensuring the high dispersion of Pt. The mass activity of Pt-based catalysts is usually used to evaluate the catalytic performance of MOR, and it can be found that the mass activity of Pt (16%)/Ni_3Fe_1-LDHs for MOR is as high as 999 mA mg_{Pt}^{-1}, which is 1.23 times higher than that of the commercial Pt/C (781 mA mg_{Pt}^{-1}). The NiFe-LDHs substrate further enhances the resistance to poisoning and maintain stability after 200,000 s of cycling tests. Therefore, methods such as doping, single-atom regulation, and constructing internal electric fields can achieve good MOR activity. However, intermediates generated during methanol oxidation may cause catalyst poisoning, affecting long-term stability.

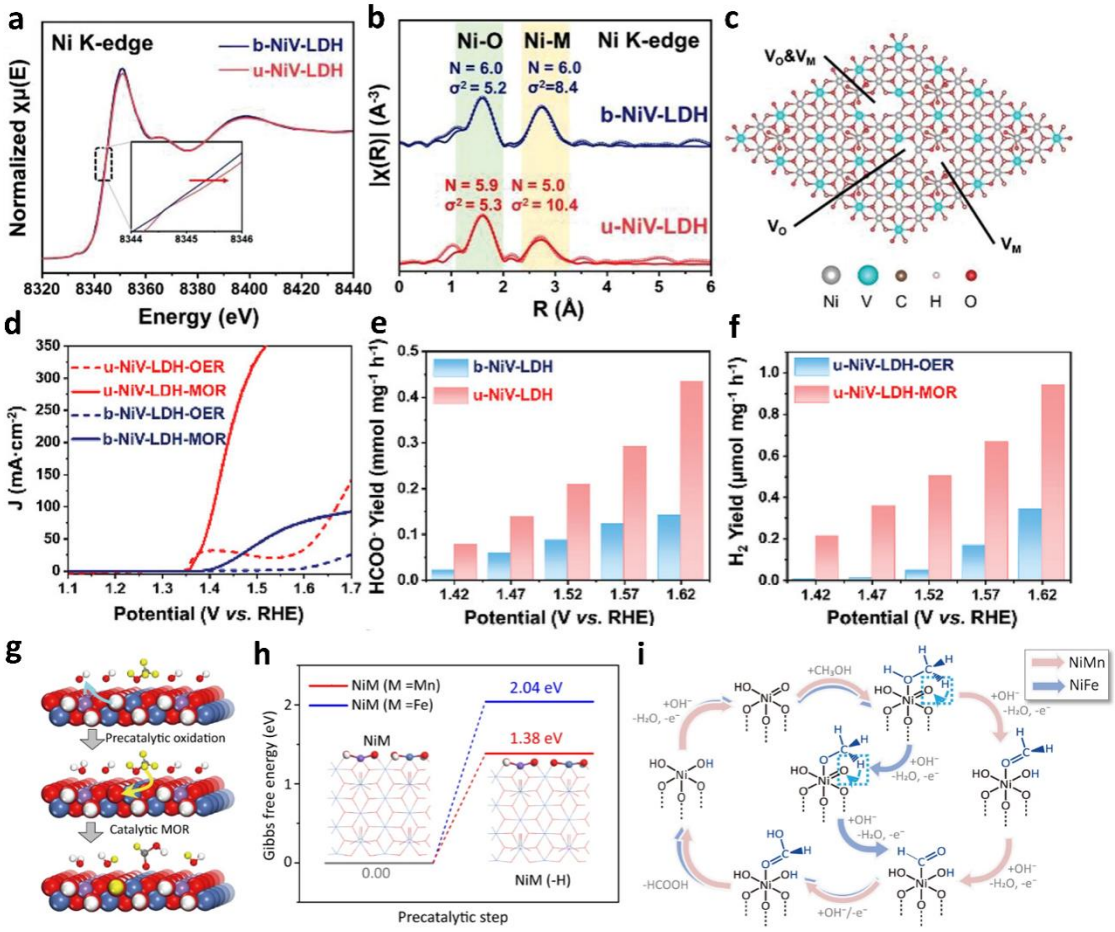

Figure 3. (**a**) Ni K-edge XANES spectra. (**b**) Ni K-edge EXFAS. (**c**) Defect structure of u-NiV-LDH. (**d**) LSV curves. (**e**) Formic acid yield. (**f**) Cathodic H_2 yield. (**a**–**f**) Reprinted with permission from [54]. Copyright 2024 Wiley-VCH GmbH. (**g**) Reaction scheme for the overall MOR on NiM-LDHs (M = Mn, Fe). (**h**) Precatalytic MOR process. (**i**) An unconventional bifunctional mechanism proposed for the overall MOR process. (**g**–**i**) Reprinted with permission from [56]. Copyright 2023 Springer Nature.

Reaction Mechanism of Methanol Oxidation to Formic Acid: To investigate the mechanism underlying the high MOR activity of LDH-based catalysts, a combined study using H/D kinetic isotope effect (KIE) measurements and density functional theory (DFT) calculations was employed. Feng et al. [56] proposed a cyclic pathway that consisted of reversible redox transitions of Ni^{II}-$(OH)_2$/Ni^{III}-OOH during MOR processes. To be consistent with experimental results and simplify the computational model, single-electron oxidation (Equation

(8)) was used to generate Ni^{III}-OOH on the LDH model surface (Figure 3g), the oxidation product (i.e., NiM hydroxyl oxide) is denoted as NiM(-H) (M = Mn, Fe). Subsequently, DFT calculations revealed a pathway starting with methanol adsorption (Equation (9)) on the Ni site of the Ni^{III}-OOH species, followed by a series of dehydrogenation reactions (Equations (10) and (11)), ultimately forming formic acid (Equation (12)): [22,57]

$$NiM + OH^- \rightarrow NiM(-H) + H_2O + e^- \quad (8)$$

$$NiM(-H) /* + CH_3OH \rightarrow NiM(-H) /*CH_3OH \quad (9)$$

$$NiM(-H) /*CH_3OH + OH^- \rightarrow NiM(-H) /*OCH_2 + H_2O(l) + e^- \quad (10)$$

$$NiM /*OCH_2 + OH^- \rightarrow NiM(-H) /*CHO + H_2O(l) + e^- \quad (11)$$

$$NiM /*CHO + OH^- \rightarrow NiM(-H) /*HCOOH + e^- \quad (12)$$

The differences in catalytic performance between NiMn and NiFe-LDHs can be attributed to their distinct Ni^{II}-$(OH)_2$/Ni^{III}-OOH oxidation behaviors, which lead to either non-spontaneous or spontaneous MOR processes (Figure 3h,i). Therefore, this study provides a clear understanding of the MOR mechanism of nickel-based LDHs and can be extended to the electrooxidation of various primary and secondary alcohols. Song et al. demonstrated that a NiFe-LDH/NiFe-ethylaminobenzene (NiFe-LDH/NiFe-HABx) exhibits excellent catalytic performance for methanol oxidation to formic acid, with the faradaic efficiency for formic acid products approaching 100% [58]. Importantly, theoretical calculations indicate that electrons transfer from NiFe-HAB to NiFe-LDH at interface tailors the electronic structure of NiFe-LDH, which not only passivates the OER during MOR but also facilitates the adsorption for methanol for MOR [59,60].

However, although the electrocatalytic selective oxidation of alcohol molecules coupled with hydrogen production can significantly enhance the overall efficiency of water splitting and yield high-value chemicals, the molecular-level insights into the electrocatalytic MOR process are still lacking. Additionally, monitoring the complex chemical transformations and the evolution of active sites during catalysis requires further exploration.

5-Hydroxymethylfurfural Oxidation Reaction to 2,5-furandicarboxylic Acid: 5-Hydroxymethylfurfural (HMF) is a biomass-derived compound with significant application potential and holds broad prospects in the field of biomass valorization [61]. HMF contains hydroxyl and aldehyde groups, which can be selectively oxidized to 2,5-furandicarboxylic acid (FDCA) or even further oxidized to the furan ring using appropriate catalysts [62]. For example, when both the aldehyde and hydroxyl groups are oxidized simultaneously, FDCA is obtained. Oxidation of the aldehyde group alone results in 5-hydroxymethylfurfural-2-carboxylic acid (HMFCA), while oxidation of the hydroxyl group alone yields 2,5-furandicarboxaldehyde (DFF) [63]. FDCA has significant potential as a sustainable substitute for terephthalic acid, with promising applications in pharmaceutical packaging, engineering plastics, nylon production, coatings, and plasticizers. In recent years, non-precious metal-based catalysts have been extensively applied in the field of HMF oxidation due to their good catalytic activity, and cost-effectiveness. Shao et al. [64] reported an integrated efficient electrocatalyst for the oxidation of 5-hydroxymethylfurfural (HMF) based on ultrathin CoAl-LDH nanosheet array (E-CoAl-LDH-NSA) with abundant oxygen vacancies (Figure 4a). Benefiting from large electrochemical surface area and abundant oxygen vacancies, the ultrathin E-CoAl-LDH-NSA shows excellent electrocatalytic activity for HMF oxidation, with a low onset potential of 1.30 V vs. RHE (Figure 4b), and a high FE of over 95% in wide potential window of 1.42 to 1.57 V vs. RHE (Figure 4c). Recent reports suggest that introducing single atoms on the surface of LDHs not only maximizes atomic utilization efficiency but also obtain a large number of active sites. Li et al [65]. loaded single Ru atoms onto NiFe-LDH ($Ru_{0.3}$/NiFe) using a two-step electrodeposition method, which further enhanced the adsorption capability and selective oxidation of HMF by the LDH catalysts. The $Ru_{0.3}$/NiFe showed extremely low overpotential (243 mV at 10 mA cm^{-2}) and excellent HMF conversion (99.43%), FDCA selectivity (99.24%) and yield (98.68%) in HMFOR (Figure 4d,e). Although the oxidation activity of HMF has greatly improved in recent years, the catalytic activity and stability of non-precious metal catalysts such as LDHs still require further enhancement.

Reaction Mechanism of 5-hydroxymethylfurfural Oxidation Reaction to 2,5-furandicarboxylic Acid: Nicholas M. Bedford, et al., investigated the HMFOR mechanism based on introducing oxygen vacancies (V_O) into NiFe-LDH nanosheets through Ce and La doping (Ce-NiFe-V_O) [20]. They found that the HMFOR has three fundamental reaction steps (HMF → HMFCA → FFCA → FDCA), the second reaction step (i.e., *FFCA chemisorption) is endothermic process, acting as the rate-limiting step for LDHs-based electrocatalysts. Particularly, the change in reaction free energy for HMFCA → FFCA on Ce-NiFe-V_O (1.41 eV) is lower than those on Ce-NiFe (1.54 eV), NiFe (1.71 eV) and La-NiFe (1.74 eV) (Figure 4f). Therefore, V_O in Ce-NiFe enhance

M-O covalency, preferentially attracting OH^- to these sites and reducing competitive adsorption of OH^- and HMF at the same active sites (Figure 4g). Sun et al. reported a bimetallic Ni-Cu electrocatalyst supported on nickel foam (Ni-Cu/NF) to passivate the OER process while the oxidation of HMF is significantly enhanced. A current density of 1000 mA cm^{-2} can be achieved at 1.50 V vs. RHE [66]. In situ EIS and Raman spectroscopy revealed that NiOOH is the active site for HMF oxidation [67,68]. Although the activity and selectivity for HMF oxidation have been significantly improved, different transition metals have various effects on catalytic activity and HMFOR. Further research into the structure-performance relationship of transition metal catalysts is still needed to enhance both efficiency and selectivity.

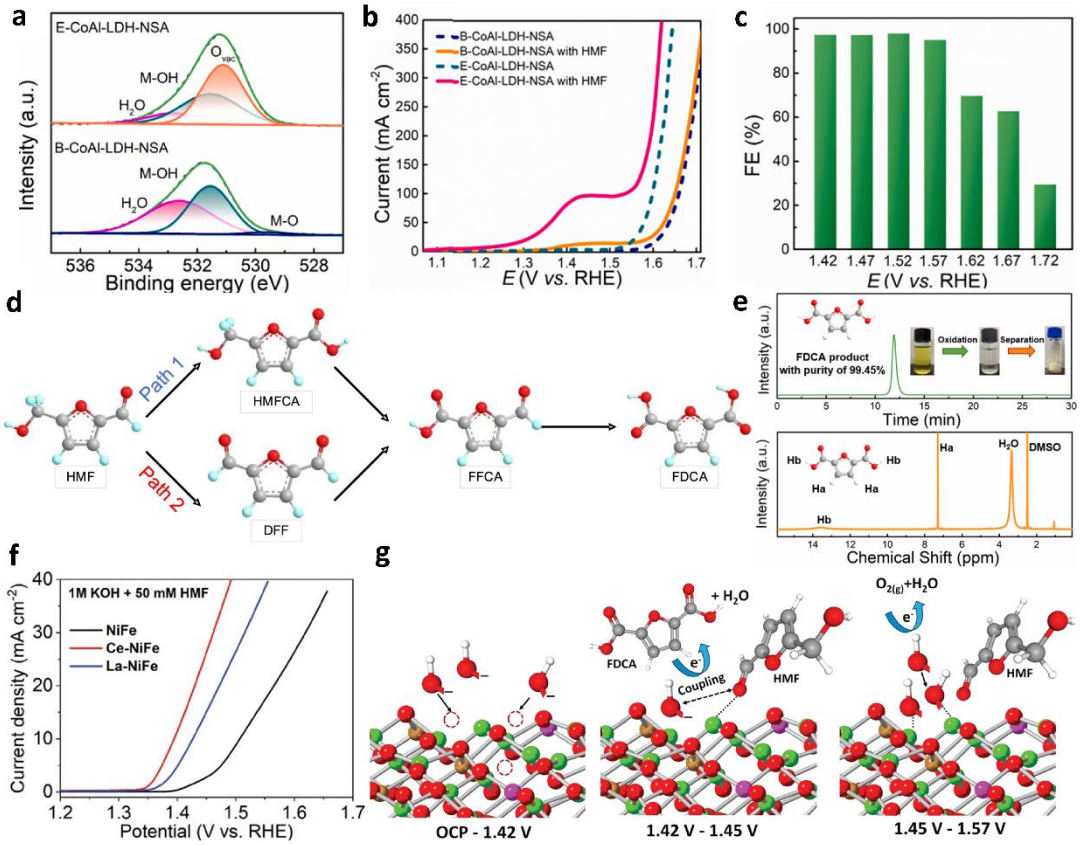

Figure 4. (**a**) Co 2*p* XPS spectra. (**b**) LSV curves. (**c**) FE of FDCA under different potentials. (**a**–**c**,**e**) Reprinted with permission from [64]. Copyright 2021 Elsevier. (**d**) Two path ways for the oxidation of HMF to produce FDCA. (**d**) Reprinted with permission from [65]. Copyright 2023 Elsevier. (**e**) HPLC chromatogram spectra and ^{1}H NMR spectra of the FDCA product. (**f**) LSV curves. (**g**) Scheme of structure-activity relationships as a function of applied potential in Ce-NiFe. (**f**,**g**) Reprinted with permission from [20]. Copyright 2024 Wiley-VCH GmbH.

4.2. Electrocatalytic Molecular Oxidation for Pollutants Degradation

In addition to the application of LDH materials for small molecule oxidation to produce high-value chemicals and in dual electrolyzer systems for hydrogen production with cathodic HER, LDH materials can also degrade organic pollutants through LDH anodes. Reactions such as the electrocatalytic oxidation of hydrazine (N_2H_4), urea ($CO(NH_2)_2$), and sulfide ions (S^{2-}) have thermodynamic potentials significantly lower than the 1.23 V vs. RHE required for OER [69,70]. Combining urea and hydrazine wastewater electrocatalytic degradation with water splitting shows significant potential for addressing environmental issues and producing high green energy for applications such as direct urea and direct hydrazine fuel cells, despite the lower economic value of the reaction products.

Electrocatalytic Hydrazine Oxidation, Degradation and Reaction Mechanism: Hydrazine is a toxic compound commonly found in pharmaceutical and petrochemical wastewater. Inhalation of hydrazine can lead to severe health issues, including blood abnormalities, permanent DNA damage, and organ damage [19]. When hydrazine-containing wastewater is discharged into water bodies, it can harm aquatic life and deplete dissolved oxygen, leading to deteriorated water quality. At the same time, hydrazine is an important chemical reagent, widely used in organic synthesis and inorganic compounds production, rocket fuel. Recently, modified LDH materials

have demonstrated significant potential for replacing OER in the HzOR. Wu et al. developed an in-situ growth of nitrogen-doped NiZnCu layered double hydroxides (N-NiZnCu LDH/rGO) on nickel foam, show that at a current density of 10 mA cm^{-2}, the voltages of AOR, UOR, and HzOR are 0.49 V, 1.31 V, and 0.01 V with a high stability (over 3000 CV cycles), which are much better than those of Pt/C [71]. This demonstrates that N-NiZnCu LDH/rGO can replace precious metals in commercial hydrogen production through water splitting and is also suitable for industrial wastewater treatment. Liu et al. prepared a Pd species-loaded NiFe-LDH, where the Pd NCs/NiFe catalyst exhibited a current density of 4.3 A mg Pd^{-1} at 0.35 V vs. RHE (Figure 5a). This is one of the most effective HzOR catalysts reported to date. The LSV curves reveal that the NiFe substrate shows no catalytic activity for N_2H_4, indicating that the active sites are the Pd species. At 0.35 V, the Pd SA/NiFe catalyst demonstrates the highest current density of 4.3 A mg Pd^{-1} which is 36 times higher than Pd SA/NiFe and 7 times higher than Pd NPs/NiFe [72]. It also exhibits the best reaction kinetics and an electrochemical impedance approaching that of precious metals (Figure 5b,c). Therefore, strategies like element doping, lattice strain engineering, and the creation of single-atom active sites can significantly accelerate the hydrazine oxidation reaction. Furthermore, a hydrazine oxidation-assisted water-splitting electrolyzer offers an energy-efficient alternative to traditional water-splitting systems (Figure 5d,e). However, the HzOR reaction generates a large volume of N_2 gas, which can lead to bubble adhesion and potentially damage the catalyst during operation.

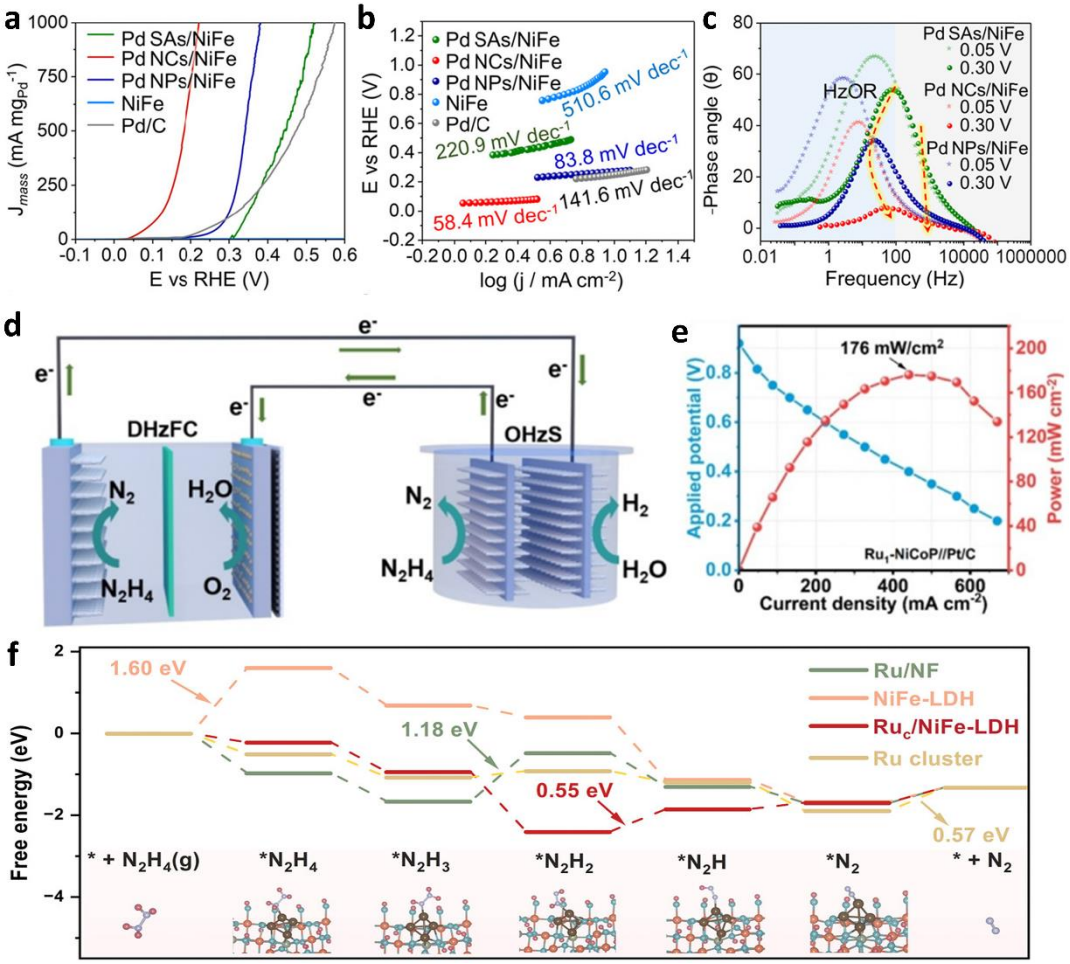

Figure 5. (**a**) LSV curves for N_2H_4 oxidation. (**b**) Tafel plots. (**c**) Bode plots. (**a**–**c**) Reprinted with permission from [72]. Copyright 2022 American Chemical Society. (**d**) A self-powered hydrogen production system integrated by driving the OHzS electrolyzer with DHzFC as power supply, and the corresponding discharge polarization curve and power density plot (**e**). (**d**,**e**) Reprinted with permission from [73]. Copyright 2023 Wiley-VCH GmbH. (**f**) The calculated Gibbs free energy. (**f**) Reprinted with permission from [74]. Copyright 2024 Wiley-VCH GmbH.

The theoretical potential for hydrazine oxidation can be as low as −0.33 V vs. RHE. Developing efficient and cost-effective bifunctional electrocatalysts for both HzOR and HER is crucial for advancing electrolytic systems. Recently, there has been further exploration into the reaction mechanisms of efficient hydrazine oxidation catalysts: Song et al. prepared Pd NCs/NiFe catalysts, and the electrons transfer from Pd species to NiFe-LDH supports, and the Pd NCs/NiFe exhibited the most positive valence state and the highest *d* band center due to the uplifting of

empty 5*d* orbitals originating from the presence of strong intracluster interactions and formation of the Pd−Pd bonds, which led to strong interaction with hydrazine [73]. Additionally, Zhang et al. designed Ru anchoring on NiFe-LDH (Ru_c/NiFe-LDH) by forms the Ru-O-Ni/Fe bridge between Ru atoms and LDH support. They found that the electrocatalytic oxidation of hydrazine follows six reaction steps: $N_2H_4 \rightarrow *N_2H_4 \rightarrow *N_2H_3 \rightarrow *N_2H_2 \rightarrow *N_2H \rightarrow *N_2 \rightarrow N_2$. The Ru−O−Ni/Fe bridge in Ru_c/NiFe-LDH modifies the coordination environment and lowers the *d*-band center [74]. This results in improved intermediate adsorption/desorption energies on the Ru surface, leading to superior catalytic performance (Figure 5f). Although DFT calculations can now demonstrate the reaction pathways and energy barriers of catalysts, identifying the true active sites and key intermediates in the HzOR reaction. Future work should focus on developing advanced in situ characterization techniques and isotope labeling to analyze key intermediates and actual catalytic species in real time.

Electrocatalytic Urea Oxidation, Degradation and Reaction Mechanism: Urea, abundant in industrial wastewater as well as human and animal urine, usually lead to the contamination of rivers, lakes, and groundwater sources [75,76]. Additionally, high levels of ammonia nitrogen and nitrates can cause poisoning and death in fish and shellfish, posing risks to human health through the food chain [77]. Therefore, there is an urgent need to develop highly selective and active urea oxidation reaction (UOR) catalysts. On one hand, the thermodynamic potential for UOR is significantly lower than that for OER, making it a cost-effective and widely applicable organic substrate in agriculture and pharmaceuticals [78]. On the other hand, urea electrochemical oxidation is beneficial for treating urea-containing wastewater [79]. Moreover, LDHs-class catalysts also show strong long-term stability during the UOR reaction process, which is conducive to the efficient operation of catalysts in the long term. Huang et al. successfully prepared a composite material composed of α-FeOOH and NiFe-based LDH, and stable NiOOH is obtained by the following electro-oxidation method. Due to the strong electron-capturing ability of α-FeOOH, the charge redistribution around the Ni/Fe sites is effectively facilitated, thereby activating the Ni atoms in the LDH [80]. Simultaneously, the optimization of the *d*-band center balances the absorption and desorption energies, significantly lowering the Gibbs free energy barriers for both the OER and UOR. Consequently, this results in an outstanding overpotential of 195 mV and a potential of 1.35 V at 10 mA cm^{-2}. Additionally, constructing heterostructures is another effective strategy for achieving high-efficiency UOR. Wu et al. created ultrafine homogenous Ni_2P-Co_2P heterostructures (Ni_2P-Co_2P/C) from a Ni-Co LDH on a single nanosheet. It requires only an ultralow overpotential of 1.27 V to achieve a current density of 10 mA cm^{-2}, with a Tafel slope of just 28.71 mV dec^{-1}. This performance is attributed to the interfacial synergy between the two components and the ultra-hydrophilic/ultra-phobic surface properties [81]. Additionally, when Ni_2P-Co_2P replaces the anode OER in the Pt/C system for urea wastewater purification while producing hydrogen, the UOR/HER system requires only a cell voltage of 1.41 V to drive a current density of 100 mA cm^{-2}, which is 352 mV lower than that of conventional water electrolysis systems. Strategies such as incorporating single atoms, creating oxygen vacancies, and introducing defects are also employed to enhance UOR selectivity and activity. However, the activity and stability of currently reported UOR catalysts still fall short. Transition metal Ni-based catalysts show significant potential, but their stability is often compromised by issues such as CO poisoning and inevitable metal corrosion and dissolution.

The UOR can simultaneously remove urea and enable energy-efficient hydrogen production (via urea-assisted water splitting) or power generation (through direct urea fuel cells). This advantage arises because UOR is thermodynamically more favorable than the anode OER, with a fuel cell potential of 0.37 V (Equation 13), significantly lower than the conventional water splitting potential of 1.23 V (Equation (14)). Moreover, the oxidation products of urea are CO_2 and N_2 (Equation (15)) [82]. However, due to the complex six-electron transfer process, UOR inherently experiences slow kinetics, necessitating high-performance catalysts to enhance the reaction rate.

$$4OH^- \rightarrow H_2O + O_2 + 4e^- \quad (13)$$

$$CO(NH_2)_2 + 6OH^- \rightarrow CO_2 + 5H_2O + N_2 + 6e^- \quad (14)$$

$$6H_2O + 6e^- \rightarrow 3H_2 + 6OH^- \quad (15)$$

To further elucidate the kinetics of the urea oxidation reaction (UOR), Huang et al. evaluated absorption energy of urea in three coordination (bridge coordination, oxygen coordination, nitrogen coordination) was assessed (Figure 6a–d). The best adsorption mode on NiOOH is oxygen-coordinated (−1.15 eV), while on FeOOH/NiOOH is nitrogen coordinated urea (−1.25 eV) [83]. Therefore, FeOOH/NiOOH possesses the most negative adsorption energy, accelerating the urea to absorb on the catalyst. Theoretically, the formation of N_2 occurs through the key molecular N-N coupling reaction during the stepwise dehydrogenation of urea. However,

the weakening of the C=N bond can lead to its cleavage into cyanate (NCO^-) and $*NH_x$, which can subsequently be overoxidized to secondary NO_x^- species (Figure 6a) [83]. Therefore, it is crucial to prevent the cleavage of the C=N bond in urea to ensure its selective conversion to N_2. Peng et al [84]. also analyzed the catalytic mechanism of UOR and HER using DFT calculation based on Fe-$Co_{0.85}Se$/FeCo LDH. They found that the local interaction of interfacial Co-Se/O-Fe bonds modulates the electronic structure, improves the reactive kinetics and intrinsic activity for HER and UOR (Figure 6e,f). Moreover, the research of Peng's group implies that the importance steps for UOR is $CO(NH_2)_2 \rightarrow CO(NH_2)_2* \rightarrow HNCO(NH_2)* \rightarrow NCO* + NH*$, while lacks of experimental results to verify these reaction processes. Future efforts should focus on expanding the application of urea oxidation, particularly in industrial wastewater treatment and advanced sensor technologies, to demonstrate its potential in addressing pressing environmental and energy challenges.

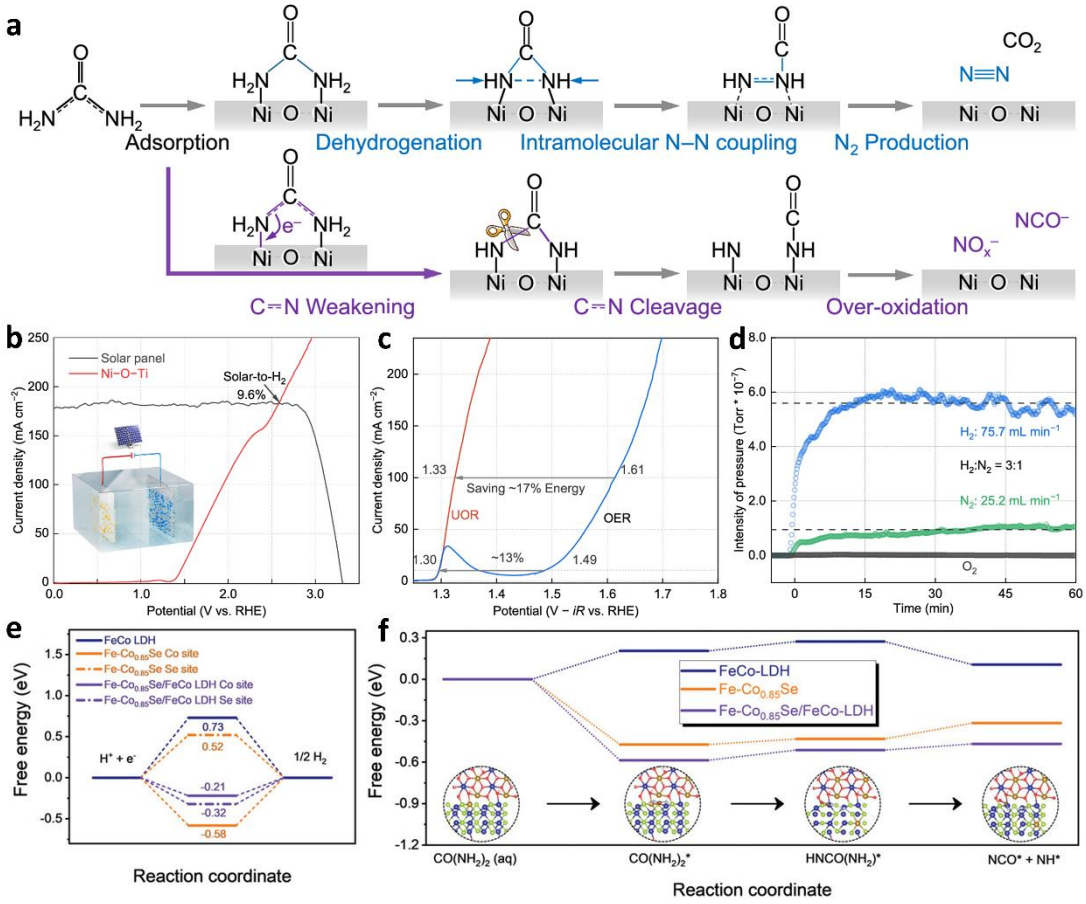

Figure 6. (**a**) The UOR pathways for N_2/CO_2 or NO_x^-/NCO^- production on connected symmetric Ni-O-Ni sites. (**b**) J-V curve. (**c**) LSV curves. (**d**) The on-line MS of H_2 and N_2/O_2 collected from cathode and anode chambers. (**a**–**d**) Reprinted with permission from [83]. Copyright 2024 Springer Nature. (**e**) Calculated hydrogen adsorption energy. (**f**) Free energy diagrams of the simplified UOR. (**e**,**f**) Reprinted with permission from [84]. Copyright 2023 Wiley-VCH GmbH.

4.3. Electrocatalytic Oxidation of the Other Small Molecular

Other thermodynamically favorable small molecules, such as ethanol, benzyl alcohol, chitosan, toluene, amines, glucose, and sulfide ions, have also been explored for electrocatalytic oxidation as alternatives to OER for energy-efficient hydrogen production. The thermodynamically advantageous ethanol oxidation reaction (EOR) instead of the anodic OER is considered to be a promising method for achieving both energy-efficient hydrogen production and high-value chemical production (e.g., acetic acid). Huang et al [85]. designed single-atom In-doped sub-nanometer Pt nanowires (SA In-Pt NWs) as high-performance electrocatalysts for HER and EOR across a full pH range. They achieve 10 mA cm^{-2} with a low overpotential of just 0.62 V and exhibit a high Faradaic efficiency of 93%, enabling the conversion of ethanol to valuable acetic acid in the anode of a fuel cell. Qiu et al [86]. was the first to prepare nickel-cobalt hydroxide nanosheets (A-Ni-Co-H/NF) supported on nickel foam. The A-Ni-Co-H/NF feature a large active surface area and low charge transfer resistance, enabling the electrocatalytic production and separation of pure benzoic acid, and industrial-scale current densities in excess of 400 mA cm^{-2} were achieved

without OER, with Ph-COOH yields approaching 100%. Shi et al [87]. successfully developed an amorphous high-entropy catalyst for the sulfur oxidation reaction (SOR). At a low potential of 0.25 V, it delivers a current density of 100 mA cm^{-2} and maintains stable electrolysis for 100 h at a high current density of 1000 mA cm^{-2}. This performance is attributed to the tuning of the chemical environment around the active sites by metal cations of varying softness and hardness, which synergistically enhances the adsorption and desorption processes of sulfide ions during SOR. Although various small molecule oxidation technologies have made significant strides recently, there remains substantial potential for improving electrocatalytic activity. There is still a need for well-designed, efficient, and stable catalysts.

6. Summary and Outlook

In recent years, there has been growing interest in using electrocatalytic small molecule oxidation to synthesize high-value chemicals or degrade pollutants as an alternative to the kinetically sluggish OER reaction. This review summarizes recent advances in LDH-based catalysts for the electrocatalytic oxidation of various small molecules, including alcohol, aldehyde, hydrazine, urea, and sulfide. It covers strategies such as doping, heterojunction construction, and morphology optimization to enhance catalytic performance. This coupling mechanism not only enables the production of high-value chemicals and pollutant degradation at the anode but also allows hydrogen production from mixed electrolytic water at significantly reduced voltages. We try to unearth the most important factors that affect the catalytic performance of electrocatalytic small molecule oxidations, nevertheless, significant effort is still needed to fundamentally understand the reaction mechanism and to further enhance the reaction kinetics (Table 1). However, we believe that LDHs materials show great potential for energy conversion and catalysis, and their unique layered structure and ion-exchange ability make them excellent candidates for high-performance electrocatalysts. Research should focus on the development of new synthesis methods and modification strategies to improve the stability, durability and cost-effectiveness of LDHs-based catalysts. Several key challenges remain to be addressed for the industrialization of LDH-based catalysts for electrocatalytic small molecule oxidation. (1) Some electrocatalysts exhibits high performance for individual reactions but only at low current densities. (2) The mechanism of anodic small molecule oxidation is still controversial. (3) Effective separation of many high-value chemicals remains challenging.

Table 1. List of parameters affecting the activities of electrocatalytic typical small molecule oxidation.

Samples	Reaction	Active Sites	Coordination Number	d-Band Center	Nanostructure	Ref.
u-NiV-LDH	MOR	Ni	5.1	−1.27	nanosheets	[48]
Pt/NiFe-LDH	MOR	Pt	—	—	nanosheets	[49]
NiMn-LDH	MOR	Mn	—	−2.75	nanoparticle	[50]
NiFe-LDH/NiFe-HAB	MOR	Fe	—	—	nanosheets	[52]
E-CoAl-LDH-NSA	HMFOR	Co	3.7	~−1.8	nanoplatelets	[58]
Ru/NiFe-LDH	HMFOR	Ru	3.8	—	nanosheets	[59]
Ce-NiFe-LDH	HMFOR	Ce	2.05	—	nanoparticle	[20]
(Ni-Cu/NF)	HMFOR	Ni, Cu	—	—	nanosheets	[60]
Pd NCs/NiFe	HzOR	Pt	3	−1.76	nanoparticle	[66]
Ru_1- NiCoP	HzOR	Ru	6	−1.10	nanoparticle	[67]
Ru_c- NiCoP	HzOR	Ru	—	−1.74	nanoparticle	[68]
LDH/α-FeOOH	UOR	Ni	6	−1.77	nanosheets	[74]
Ni_2P–Co_2P/C	UOR	Co	—	−1.12	nanosheets	[75]
Ni-O-Ti	UOR	Ni	5	—	nanoparticle	[77]
Fe-$Co_{0.85}$Se/FeCo LDH	UOR	Co	—	−1.48	nanosheets	[78]

(1) Reaction Mechanism: Currently, the mechanisms of various small molecule oxidation reactions are still debated. Future research should employ advanced in-situ characterization techniques, such as in-situ diffuse reflectance Fourier-transform infrared spectroscopy, in-situ electron spin resonance spectroscopy, in-situ X-ray photoelectron spectroscopy, in situ transmission electron microscopy, and in-situ Raman spectroscopy. These methods can track changes in composition, structure, and electronic properties to explore the true reaction pathways and active sites. Additionally, DFT calculations should be used to demonstrate the energy barriers of each reaction step and identify the rate-determining step.

(2) Catalyst Design: Rational design of catalysts has always been a prerequisite for achieving high activity and stability in reactions. Controlling the nanostructure and coordination environment of catalysts is crucial for influencing reaction performance. Techniques such as crystal facet engineering, surface customization, defect engineering, structural modulation, and heterojunction design can achieve precise control over these aspects.

However, the design of small molecule oxidation catalysts still lacks specificity. A deeper understanding of the reaction mechanisms for each small molecule oxidation is needed to achieve targeted designs that optimize catalytic activity. Additionally, most small molecule oxidation electrocatalysts currently provide low current densities (<300 mA cm^{-2}) in laboratory settings. To meet the demands of industrial-scale production, future research should focus on developing electrocatalysts that can deliver higher current densities (>1000 mA cm^{-2}) and exhibit enhanced stability.

(3) Product Separation: Separating and purifying valuable products from the anode is a crucial step in industrial production. For different small molecules, suitable separation methods should be chosen, such as high-performance liquid chromatography, supercritical fluid chromatography, and membrane separation techniques. Additionally, it is important to reduce the costs of subsequent separation and purification while improving durability for long-term operation. The cost of the electrocatalysts should also be considered, including expenses related to raw materials, preparation processes, transportation, and environmental impact. Future work should focus on using abundant earth elements, simple preparation strategies, locally sourced materials, and environmentally friendly practices.

Author Contributions: S.P.J., J.L and R.L. conceived and designed the project. They also revised the article. J.L. and Z.-Q.G. wrote and revised the article, C.C. and C.W. revised the article.

Funding: This work was supported by Foshan Xianhu Labo-ratory (XHD2024-31000000-06 and XHD2021-001), Natural Science Foundation of China (No. 22308070), Guangdong Basic and Applied Basic Research Foundation (2022A1515140012) and Open Access publishing facilitated by Curtin University, as part of the Wiley–Curtin University agreement via the Council of Australian University Librarians.

Data Availability Statement: Data sharing is not applicable to this article as no new data were created or analyzed in this study.

Conflict of Interests: The author declares no conflict of interest.

References

1. Khan, M.A.; Al-Attas, T.; Roy, S.; Rahman, M.M.; Ghaffour, N.; Thangadurai, V.; Larter, S.; Hu, J.; Ajayan, P.M.; Kibria, M.G. Seawater electrolysis for hydrogen production: a solution looking for a problem? *Energy Environ. Sci.* **2021**, *14*, 4831–4839. https://doi.org/10.1039/d1ee00870f.
2. Li, J.; Wang, X.; Fang, H.; Guo, X.; Zhou, R.; Wang, C.; Li, J.; Ghazzal, M.N.; Rui, Z. Unraveling the role of surface and interfacial defects in hydrogen production to construct an all-in-one broken-gap photocatalyst. *J. Mater. Chem. A* **2023**, *11*, 25639–25649. https://doi.org/10.1039/d3ta03079b.
3. Zhao, X.; Wu, G.; Zheng, X.; Jiang, P.; Yi, J.d.; Zhou, H.; Gao, X.; Yu, Z.Q.; Wu, Y. A Double Atomic-Tuned RuBi SAA/Bi@OG Nanostructure with Optimum Charge Redistribution for Efficient Hydrogen Evolution. *Angew. Chem. Int. Ed.* **2023**, *62*, e202300879. https://doi.org/10.1002/anie.202300879.
4. Li, J.; Ping Jiang, S. Small Molecule Oxidation Facilitated Seawater Splitting for Hydrogen Production: Opportunities and Challenges. *ChemCatChem* **2024**, e202400258. https://doi.org/10.1002/cctc.202400258.
5. Liu, H.; Zhang, Z.; Fang, J.; Li, M.; Sendeku, M.G.; Wang, X.; Wu, H.; Li, Y.; Ge, J.; Zhuang, Z.; et al. Eliminating over-oxidation of ruthenium oxides by niobium for highly stable electrocatalytic oxygen evolution in acidic media. *Joule* **2023**, *7*, 558–573. https://doi.org/10.1016/j.joule.2023.02.012.
6. Yang, G.; Jiao, Y.; Yan, H.; Xie, Y.; Wu, A.; Dong, X.; Guo, D.; Tian, C.; Fu, H. Interfacial Engineering of MoO_2-FeP Heterojunction for Highly Efficient Hydrogen Evolution Coupled with Biomass Electrooxidation. *Adv. Mater.* **2020**, *32*, 20000455. https://doi.org/10.1002/adma.202000455.
7. Lee, S.-Y.; Kim, I.-S.; Cho, H.-S.; Kim, C.-H.; Lee, Y.-K. Resolving Potential-Dependent Degradation of Electrodeposited $Ni(OH)_2$ Catalysts in Alkaline Oxygen Evolution Reaction (OER): In Situ XANES Studies. *Appl. Catal. B Environ.* **2021**, *284*, 119729. https://doi.org/10.1016/j.apcatb.2020.119729.
8. Hu, S.; Feng, C.; Wang, S.; Liu, J.; Wu, H.; Zhang, L.; Zhang, J. Ni_3N/NF as Bifunctional Catalysts for Both Hydrogen Generation and Urea Decomposition. *ACS Appl. Mater. Interfaces* **2019**, *11*, 13168–13175. https://doi.org/10.1021/acsami.8b19052.
9. Tanabe, Y.; Ito, Y.; Sugawara, K.; Jeong, S.; Ohto, T.; Nishiuchi, T.; Kawada, N.; Kimura, S.; Aleman, C.F.; Takahashi, T.; et al. Coexistence of Urbach-Tail-Like Localized States and Metallic Conduction Channels in Nitrogen-Doped 3D Curved Graphene. *Adv. Mater.* **2022**, *34*, 2205986. https://doi.org/10.1002/adma.202205986.
10. Zhang, X.; Hui, L.; Yan, D.; Li, J.; Chen, X.; Wu, H.; Li, Y. Defect Rich Structure Activated 3D Palladium Catalyst for Methanol Oxidation Reaction. *Angew. Chem. Int. Ed.* **2023**, *62*, e202308968. https://doi.org/10.1002/anie.202308968.
11. Wang, Q.; Chen, L.; Guan, S.; Zhang, X.; Wang, B.; Cao, X.; Yu, Z.; He, Y.; Evans, D.G.; Feng, J.; et al. Ultrathin and Vacancy-Rich CoAl-Layered Double Hydroxide/Graphite Oxide Catalysts: Promotional Effect of Cobalt Vacancies and Oxygen Vacancies in Alcohol Oxidation. *ACS Catal.* **2018**, *8*, 3104–3115. https://doi.org/10.1021/acscatal.7b03655.

12. Ge, Z.Q.; Li, J.; Zhang, H.J.; Liu, C.; Che, G.; Liu, Z.Q. p–d Orbitals Coupling Heterosites of Ni_2P/NiFe-LDH Interface Enable O-H Cleavage for Water Splitting. *Adv. Funct. Mater.* **2024**, *34*, 2411024. https://doi.org/10.1002/adfm.202411024.
13. Bian, X.; Zhang, S.; Zhao, Y.; Shi, R.; Zhang, T. Layered double hydroxide-based photocatalytic materials toward renewable solar fuels production. *InfoMat* **2021**, *3*, 719–738. https://doi.org/10.1002/inf2.12192.
14. Song, F.; Hu, X. Exfoliation of layered double hydroxides for enhanced oxygen evolution catalysis. *Nat. Commun.* **2020**, *11*, 2522. https://doi.org/10.1038/ncomms5477.
15. Ning, F.; Shao, M.; Xu, S.; Fu, Y.; Zhang, R.; Wei, M.; Evans, D.G.; Duan, X. TiO_2/graphene/NiFe-layered double hydroxide nanorod array photoanodes for efficient photoelectrochemical water splitting. *Energy Environ. Sci.* **2016**, *9*, 2633–2643. https://doi.org/10.1039/c6ee01092j.
16. Ren, J.; Ouyang, S.; Xu, H.; Meng, X.; Wang, T.; Wang, D.; Ye, J. Targeting Activation of CO_2 and H_2 over Ru-Loaded Ultrathin Layered Double Hydroxides to Achieve Efficient Photothermal CO_2 Methanation in Flow-Type System. *Adv. Energy Mater*. **2016**, *7*, 1601657. https://doi.org/10.1002/aenm.201601657.
17. Ren, M.; Zeng, W.; Li, Z.; Cao, S.; Liu, C.; Ouyang, S.; Zhang, T.; Cui, Y.; Yuan, H. CoAl-layered double hydroxide nanosheet-based fluorescence assay for fast DNA detection. *Spectrochim. Acta A* **2020**, *240*, 118618. https://doi.org/10.1016/j.saa.2020.118618.
18. Liu, B.; Xu, S.; Zhang, M.; Li, X.; Decarolis, D.; Liu, Y.; Wang, Y.; Gibson, E.K.; Catlow, C.R.A.; Yan, K. Electrochemical upgrading of biomass-derived 5-hydroxymethylfurfural and furfural over oxygen vacancy-rich NiCoMn-layered double hydroxides nanosheets. *Green Chem.* **2021**, *23*, 4034–4043. https://doi.org/10.1039/d1gc00901j.
19. Kim, J.S.; Kim, B.; Kim, H.; Kang, K. Recent Progress on Multimetal Oxide Catalysts for the Oxygen Evolution Reaction. *Adv. Energy Mater.* **2018**, *8*, 1702774. https://doi.org/10.1002/aenm.201702774.
20. Lang, R.; Du, X.; Huang, Y.; Jiang, X.; Zhang, Q.; Guo, Y.; Liu, K.; Qiao, B.; Wang, A.; Zhang, T. Single-Atom Catalysts Based on the Metal–Oxide Interaction. *Chem. Rev.* **2020**, *120*, 11986–12043. https://doi.org/10.1021/acs.chemrev.0c00797.
21. Chen, W.; Xie, C.; Wang, Y.; Zou, Y.; Dong, C.-L.; Huang, Y.-C.; Xiao, Z.; Wei, Z.; Du, S.; Chen, C.; et al. Activity Origins and Design Principles of Nickel-Based Catalysts for Nucleophile Electrooxidation. *Chem* **2020**, *6*, 2974–2993. https://doi.org/10.1016/j.chempr.2020.07.022.
22. Zeng, L.; Chen, Y.; Sun, M.; Huang, Q.; Sun, K.; Ma, J.; Li, J.; Tan, H.; Li, M.; Pan, Y.; et al. Cooperative Rh-O_5/Ni(Fe) Site for Efficient Biomass Upgrading Coupled with H_2 Production. *J. Am. Chem. Soc.* **2023**, *145*, 17577–17587. https://doi.org/10.1021/jacs.3c02570.
23. Li, Z.; Li, B.; Yu, M.; Yu, C.; Shen, P. Amorphous metallic ultrathin nanostructures: A latent ultra-high-density atomic-level catalyst for electrochemical energy conversion. *Int. J. Hydrog. Energy.* **2022**, *47*, 26956–26977. https://doi.org/10.1016/j.ijhydene.2022.06.049.
24. Li, L.; Zhang, L.; Gou, L.; Wei, S.; Hou, X.; Wu, L. High-performance methanol electrolysis towards energy-saving hydrogen production: Using Cu_2O-Cu decorated Ni_2P nanoarray as bifunctional monolithic catalyst. *Chem. Eng. J.* **2023**, *454*, 140292. https://doi.org/10.1016/j.cej.2022.140292.
25. Han, Y.; Wang, J.; Liu, Y.; Li, T.; Wang, T.; Li, X.; Ye, X.; Li, G.; Li, J.; Hu, W.; et al. Stability challenges and opportunities of NiFe-based electrocatalysts for oxygen evolution reaction in alkaline media. *Carbon Neutralization* **2024**, *3*, 172–198. https://doi.org/10.1002/cnl2.110.
26. Zhang, L.-C.; Chen, H.; Hou, G.-R.; Zhang, L.-Z.; Li, Q.-L.; Wu, Y.-K.; Xu, M.; Bao, S.-J. Puzzle-inspired carbon dots coupled with cobalt phosphide for constructing a highly-effective overall water splitting interface. *Chem. Commun.* **2020**, *56*, 257–260. https://doi.org/10.1039/c9cc08032e.
27. Qi, Y.-F.; Wang, K.-Y.; Sun, Y.; Wang, J.; Wang, C. Engineering the Electronic Structure of NiFe Layered Double Hydroxide Nanosheet Array by Implanting Cationic Vacancies for Efficient Electrochemical Conversion of 5-Hydroxymethylfurfural to 2,5-Furandicarboxylic Acid. *ACS Sustain. Chem. Eng.* **2021**, *10*, 645–654. https://doi.org/10.1021/acssuschemeng.1c07482.
28. Zhang, M.; Liu, Y.; Liu, B.; Chen, Z.; Xu, H.; Yan, K. Trimetallic NiCoFe-Layered Double Hydroxides Nanosheets Efficient for Oxygen Evolution and Highly Selective Oxidation of Biomass-Derived 5-Hydroxymethylfurfural. *ACS Catal.* **2020**, *10*, 5179–5189. https://doi.org/10.1021/acscatal.0c00007.
29. Tan, L.; Wang, Z.; Zhao, Y.; Song, Y.F. Recent Progress on Nanostructured Layered Double Hydroxides for Visible-Light-Induced Photoreduction of CO_2. *Chem. Asian J.* **2020**, *15*, 3380–3389. https://doi.org/10.1002/asia.202000963.
30. Moges, E.A.; Chang, C.-Y.; Tsai, M.-C.; Su, W.-N.; Hwang, B.J. Electrocatalysts for value-added electrolysis coupled with hydrogen evolution. *EES Catal.* **2023**, *1*, 413–433. https://doi.org/10.1039/d3ey00017f.
31. Song, Y.; Ji, K.; Duan, H.; Shao, M. Hydrogen production coupled with water and organic oxidation based on layered double hydroxides. *Exploration* **2021**, *1*, 20210050. https://doi.org/10.1002/exp.20210050.
32. Li, D.; Tu, J.; Lu, Y.; Zhang, B. Recent advances in hybrid water electrolysis for energy-saving hydrogen production. *Green Chem. Eng.* **2023**, *4*, 17–29. https://doi.org/10.1016/j.gce.2022.11.001.
33. Ning, C.; Bai, S.; Wang, J.; Li, Z.; Han, Z.; Zhao, Y.; O'Hare, D.; Song, Y.-F. Review of photo- and electro-catalytic multi-metallic layered double hydroxides. *Coord. Chem. Rev.* **2023**, *480*, 215008. https://doi.org/10.1016/j.ccr.2022.215008.

34. Kang, W.; Wei, R.; Yin, H.; Li, D.; Chen, Z.; Huang, Q.; Zhang, P.; Jing, H.; Wang, X.; Li, C. Unraveling Sequential Oxidation Kinetics and Determining Roles of Multi-Cobalt Active Sites on Co_3O_4 Catalyst for Water Oxidation. *J. Am. Chem. Soc.* **2023**, *145*, 3470–3477. https://doi.org/10.1021/jacs.2c11508.
35. Wang, C.; Zhai, P.; Xia, M.; Liu, W.; Gao, J.; Sun, L.; Hou, J. Identification of the Origin for Reconstructed Active Sites on Oxyhydroxide for Oxygen Evolution Reaction. *Adv. Mater.* **2023**, *35*, 2209307. https://doi.org/10.1002/adma.202209307.
36. Haase, F.T.; Bergmann, A.; Jones, T.E.; Timoshenko, J.; Herzog, A.; Jeon, H.S.; Rettenmaier, C.; Cuenya, B.R. Size effects and active state formation of cobalt oxide nanoparticles during the oxygen evolution reaction. *Nat. Energy* **2022**, *7*, 765–773. https://doi.org/10.1038/s41560-022-01083-w.
37. Andaveh, R.; Sabour Rouhaghdam, A.; Ai, J.; Maleki, M.; Wang, K.; Seif, A.; Barati Darband, G.; Li, J. Boosting the electrocatalytic activity of NiSe by introducing MnCo as an efficient heterostructured electrocatalyst for large-current-density alkaline seawater splitting. *Appl. Catal. B Environ.* **2023**, *325*, 122355. https://doi.org/10.1016/j.apcatb.2022.122355.
38. Wang, X.; Zhong, H.; Xi, S.; Lee, W.S.V.; Xue, J. Understanding of Oxygen Redox in the Oxygen Evolution Reaction. Advanced Materials 2022, 34. https://doi.org/10.1002/adma.202107956.
39. Zhou, Y.; Sun, S.; Song, J.; Xi, S.; Chen, B.; Du, Y.; Fisher, A.C.; Cheng, F.; Wang, X.; Zhang, H.; et al. Enlarged Co-O Covalency in Octahedral Sites Leading to Highly Efficient Spinel Oxides for Oxygen Evolution Reaction. *Adv. Mater.* **2023**, *35*, 2209307. https://doi.org/10.1002/adma.201802912.
40. Khatun, S.; Hirani, H.; Roy, P. Seawater electrocatalysis: activity and selectivity. *J. Mater. Chem. A* **2021**, *9*, 74–86. https://doi.org/10.1039/d0ta08709b.
41. Xu, S.; Jiao, D.; Ruan, X.; Jin, Z.; Qiu, Y.; Feng, Z.; Zheng, L.; Fan, J.; Zheng, W.; Cui, X. O-2p Hybridization Enhanced Transformation of Active γ-NiOOH by Chromium Doping for Efficient Urea Oxidation Reaction. *Adv. Funct. Mater.* **2024**, *34*, 2401265. https://doi.org/10.1002/adfm.202401265.
42. Zhang, L.; Li, L.; Liang, J.; Fan, X.; He, X.; Chen, J.; Li, J.; Li, Z.; Cai, Z.; Sun, S.; et al. Highly efficient and stable oxygen evolution from seawater enabled by a hierarchical NiMoSx microcolumn@NiFe-layered double hydroxide nanosheet array. *Inorg. Chem. Front.* **2023**, *10*, 2766–2775. https://doi.org/10.1039/d3qi00341h.
43. Zhang, L.; Zhao, H.; Xu, S.; Liu, Q.; Li, T.; Luo, Y.; Gao, S.; Shi, X.; Asiri, A.M.; Sun, X. Recent Advances in 1D Electrospun Nanocatalysts for Electrochemical Water Splitting. *Small Struct.* **2021**, *2*, 2000048. https://doi.org/10.1002/sstr.202000048.
44. Pei, Y.; Cheng, J.; Zhong, H.; Pi, Z.; Zhao, Y.; Jin, F. Sulfide-oxidation-assisted electrochemical water splitting for H_2 production on a bifunctional Cu_2S/nickel foam catalyst. *Green Chem.* **2021**, *23*, 6975–6983. https://doi.org/10.1039/d1gc01857d.
45. Wei, J.; Wang, J.; Sun, X. H_2O_2 treatment boosts activity of NiFe layered double hydroxide for electro-catalytic oxidation of urea. *J. Environ. Sci.* **2023**, *129*, 152–160. https://doi.org/10.1016/j.jes.2022.08.023.
46. Fan, H.; Jia, J.; Wang, D.; Fan, J.; Wu, J.; Zhao, J.; Cui, X. High-valence Zr-incorporated nickel phosphide boosting reaction kinetics for highly efficient and robust overall water splitting. *Chem. Eng. J.* **2023**, *455*, 140908. https://doi.org/10.1016/j.cej.2022.140908.
47. Huo, J.M.; Wang, Y.; Xue, J.N.; Yuan, W.Y.; Zhai, Q.G.; Hu, M.C.; Li, S.N.; Chen, Y. High-Valence Metal Doping Induced Lattice Expansion for M-FeNi LDH toward Enhanced Urea Oxidation Electrocatalytic Activities. *Small* **2024**, *20*, 2305877. https://doi.org/10.1002/smll.202305877.
48. Shao, W.; Wang, Q.; Huang, C.; Zhang, D. High valence state metal-ion doped Fe–Ni layered double hydroxides for oxygen evolution electrocatalysts and asymmetric supercapacitors. *Adv. Mater.* **2022**, *3*, 1816–1824. https://doi.org/10.1039/d1ma01125a.
49. Xu, X.; Ullah, H.; Humayun, M.; Li, L.; Zhang, X.; Bououdina, M.; Debecker, D.P.; Huo, K.; Wang, D.; Wang, C. Fluorinated Ni-O-C Heterogeneous Catalyst for Efficient Urea-Assisted Hydrogen Production. *Adv. Funct. Mater.* **2023**, *33*, 2303986. https://doi.org/10.1002/adfm.202303986.
50. Jiang, Z.; Song, S.; Zheng, X.; Liang, X.; Li, Z.; Gu, H.; Li, Z.; Wang, Y.; Liu, S.; Chen, W.; et al. Lattice Strain and Schottky Junction Dual Regulation Boosts Ultrafine Ruthenium Nanoparticles Anchored on a N-Modified Carbon Catalyst for H_2 Production. *J. Am. Chem. Soc.* **2022**, *144*, 19619–19626. https://doi.org/10.1021/jacs.2c09613.
51. Meng, S.; Chen, C.; Gu, X.; Wu, H.; Meng, Q.; Zhang, J.; Chen, S.; Fu, X.; Liu, D.; Lei, W. Efficient photocatalytic H2 evolution, CO2 reduction and N2 fixation coupled with organic synthesis by cocatalyst and vacancies engineering. *Appl. Catal. B Environ.* **2021**, *285*, 119789. https://doi.org/10.1016/j.apcatb.2020.119789.
52. Li, Y.; Wei, X.; Chen, L.; Shi, J.; He, M. Nickel-molybdenum nitride nanoplate electrocatalysts for concurrent electrolytic hydrogen and formate productions. *Nat. Commun.* **2019**, *10*, 5335. https://doi.org/10.1038/s41467-019-13375-z.
53. Tang, C.; Zheng, Y.; Jaroniec, M.; Qiao, S.Z. Electrocatalytic Refinery for Sustainable Production of Fuels and Chemicals. *Angew. Chem. Int. Ed.* **2021**, *60*, 19572–19590. https://doi.org/10.1002/anie.202101522.
54. Wu, Z.; Bai, S.; Shen, T.; Liu, G.; Song, Z.; Hu, Y.; Sun, X.; Zheng, L.; Song, Y.F. Ultrathin NiV Layered Double Hydroxide for Methanol Electrooxidation: Understanding the Proton Detachment Kinetics and Methanol Dehydrogenation Oxidation. *Small* **2024**, *20*, 2307975. https://doi.org/10.1002/smll.202307975.

55. Talib, S.H.; Lu, Z.; Yu, X.; Ahmad, K.; Bashir, B.; Yang, Z.; Li, J. Theoretical Inspection of M1/PMA Single-Atom Electrocatalyst: Ultra-High Performance for Water Splitting (HER/OER) and Oxygen Reduction Reactions (OER). *ACS Catal.* **2021**, *11*, 8929–8941. https://doi.org/10.1021/acscatal.1c01294.
56. Zhu, B.; Dong, B.; Wang, F.; Yang, Q.; He, Y.; Zhang, C.; Jin, P.; Feng, L. Unraveling a bifunctional mechanism for methanol-to-formate electro-oxidation on nickel-based hydroxides. *Nat. Commun.* **2023**, *14*, 1686. https://doi.org/10.1038/s41467-023-37441-9.
57. Li, S.; Ma, R.; Hu, J.; Li, Z.; Liu, L.; Wang, X.; Lu, Y.; Sterbinsky, G.E.; Liu, S.; Zheng, L.; et al. Coordination environment tuning of nickel sites by oxyanions to optimize methanol electro-oxidation activity. *Nat. Commun.* **2022**, *13*, 2916. https://doi.org/10.1038/s41467-022-30670-4.
58. Jiang, S.; Xiao, T.; Xu, C.; Wang, S.; Peng, H.Q.; Zhang, W.; Liu, B.; Song, Y.F. Passivating Oxygen Evolution Activity of NiFe-LDH through Heterostructure Engineering to Realize High-Efficiency Electrocatalytic Formate and Hydrogen Co-Production. *Small* **2023**, *19*, 2208027. https://doi.org/10.1002/smll.202208027.
59. Barwe, S.; Weidner, J.; Cychy, S.; Morales, D.M.; Dieckhöfer, S.; Hiltrop, D.; Masa, J.; Muhler, M.; Schuhmann, W. Electrocatalytic Oxidation of 5-(Hydroxymethyl)furfural Using High-Surface-Area Nickel Boride. *Angew. Chem. Int. Ed.* **2018**, *57*, 11460–11464. https://doi.org/10.1002/anie.201806298.
60. Mondal, B.; Karjule, N.; Singh, C.; Shimoni, R.; Volokh, M.; Hod, I.; Shalom, M. Unraveling the Mechanisms of Electrocatalytic Oxygenation and Dehydrogenation of Organic Molecules to Value-Added Chemicals Over a Ni–Fe Oxide Catalyst. *Adv. Energy Mater.* **2021**, *11*, 2101858. https://doi.org/10.1002/aenm.202101858.
61. Bell, E.L.; Smithson, R.; Kilbride, S.; Foster, J.; Hardy, F.J.; Ramachandran, S.; Tedstone, A.A.; Haigh, S.J.; Garforth, A.A.; Day, P.J.R.; et al. Directed evolution of an efficient and thermostable PET depolymerase. *Nat. Catal.* **2022**, *5*, 673–681. https://doi.org/10.1038/s41929-022-00821-3.
62. Zhang, Z.; Huber, G.W. Catalytic oxidation of carbohydrates into organic acids and furan chemicals. *Chem. Soc. Rev.* **2018**, *47*, 1351–1390. https://doi.org/10.1039/c7cs00213k.
63. Cai, J.; Li, K.; Wu, S. Recent advances in catalytic conversion of biomass derived 5-hydroxymethylfurfural into 2,5-furandicarboxylic acid. *Biomass Bioenergy* **2022**, *158*, 106358. https://doi.org/10.1016/j.biombioe.2022.106358
64. Song, Y.; Li, Z.; Fan, K.; Ren, Z.; Xie, W.; Yang, Y.; Shao, M.; Wei, M. Ultrathin layered double hydroxides nanosheets array towards efficient electrooxidation of 5-hydroxymethylfurfural coupled with hydrogen generation. *Appl. Catal. B Environ.* **2021**, *299*, 120669. https://doi.org/10.1016/j.apcatb.2021.120669.
65. Cai, Z.; Wang, P.; Zhang, J.; Chen, A.; Zhang, J.; Yan, Y.; Wang, X. Reinforced Layered Double Hydroxide Oxygen-Evolution Electrocatalysts: A Polyoxometallic Acid Wet-Etching Approach and Synergistic Mechanism. *Adv. Mater.* **2022**, *34*, 2110696. https://doi.org/10.1002/adma.202110696.
66. Chen, D.; Ding, Y.; Cao, X.; Wang, L.; Lee, H.; Lin, G.; Li, W.; Ding, G.; Sun, L. Highly Efficient Biomass Upgrading by a Ni−Cu Electrocatalyst Featuring Passivation of Water Oxidation Activity. *Angew. Chem. Int. Ed.* **2023**, *62*, e202309478. https://doi.org/10.1002/anie.202309478.
67. Xu, G.-R.; Batmunkh, M.; Donne, S.; Jin, H.; Jiang, J.-X.; Chen, Y.; Ma, T. Ruthenium(iii) polyethyleneimine complexes for bifunctional ammonia production and biomass upgrading. *J. Mater. Chem. A* **2019**, *7*, 25433–25440. https://doi.org/10.1039/c9ta10267a.
68. Liu, Z.; Li, Y.; Guo, H.; Zhao, J.; Zhang, H.; Song, R. Interface engineering of amorphous/crystalline heterojunctions with synergistic Ru doping for efficient hydrazine oxidation assisted overall water splitting. *J. Mater. Chem. A* **2023**, *11*, 24667–24677. https://doi.org/10.1039/d3ta05082c.
69. Zhu, Y.; He, Z.; Choi, Y.; Chen, H.; Li, X.; Zhao, B.; Yu, Y.; Zhang, H.; Stoerzinger, K.A.; Feng, Z.; et al. Tuning proton-coupled electron transfer by crystal orientation for efficient water oxidization on double perovskite oxides. *Nat. Commun.* **2020**, *11*, 4299. https://doi.org/10.1038/s41467-020-17657-9.
70. Park, M.; Gu, M.; Kim, B.-S. Tailorable Electrocatalytic 5-Hydroxymethylfurfural Oxidation and H_2 Production: Architecture–Performance Relationship in Bifunctional Multilayer Electrodes. *ACS Nano* **2020**, *14*, 6812–6822. https://doi.org/10.1021/acsnano.0c00581.
71. Hu, S.; Tan, Y.; Feng, C.; Wu, H.; Zhang, J.; Mei, H. Synthesis of N doped NiZnCu-layered double hydroxides with reduced graphene oxide on nickel foam as versatile electrocatalysts for hydrogen production in hybrid-water electrolysis. *J. Power Sources* **2020**, *453*, 227872. https://doi.org/10.1016/j.jpowsour.2020.227872.
72. Liu, G.; Nie, T.; Wang, H.; Shen, T.; Sun, X.; Bai, S.; Zheng, L.; Song, Y.-F. Size Sensitivity of Supported Palladium Species on Layered Double Hydroxides for the Electro-oxidation Dehydrogenation of Hydrazine: From Nanoparticles to Nanoclusters and Single Atoms. *ACS Catal.* **2022**, *12*, 10711–10717. https://doi.org/10.1021/acscatal.2c02628.
73. Hu, Y.; Chao, T.; Li, Y.; Liu, P.; Zhao, T.; Yu, G.; Chen, C.; Liang, X.; Jin, H.; Niu, S.; et al. Cooperative Ni(Co)-Ru-P Sites Activate Dehydrogenation for Hydrazine Oxidation Assisting Self-powered H_2 Production. *Angew. Chem. Int. Ed.* **2023**, *62*, e202308800. https://doi.org/10.1002/anie.202308800.
74. Zhu, Y.; Chen, Y.; Feng, Y.; Meng, X.; Xia, J.; Zhang, G. Constructing Ru-O-TM Bridge in NiFe-LDH Enables High Current Hydrazine-assisted H_2 Production. *Adv. Mater.* **2024**, *36*, 2401694. https://doi.org/10.1002/adma.202401694.
75. Rollinson, A.N.; Jones, J.; Dupont, V.; Twigg, M.V. Urea as a hydrogen carrier: a perspective on its potential for safe, sustainable and long-term energy supply. *Environ. Sci.* **2011**, *4*, 1216. https://doi.org/10.1039/c0ee00705f.

76. Dong, H.; Laguna, C.M.; Liu, M.J.; Guo, J.; Tarpeh, W.A. Electrified Ion Exchange Enabled by Water Dissociation in Bipolar Membranes for Nitrogen Recovery from Source-Separated Urine. *Environ. Sci. Technol.* **2022**, *56*, 16134–16143. https://doi.org/10.1021/acs.est.2c03771.
77. Urbańczyk, E.; Sowa, M.; Simka, W. Urea removal from aqueous solutions—a review. *J. Appl. Electrochem.* **2016**, *46*, 1011–1029. https://doi.org/10.1007/s10800-016-0993-6.
78. Zhang, X.; Feizpoor, S.; Humayun, M.; Wang, C. Urea oxidation reaction electrocatalysts: Correlation of structure, activity, and selectivity. *Chem Catal.* **2024**, *4*, 100840. https://doi.org/10.1016/j.checat.2023.100840.
79. Zhao, H.; Zhang, Y.; Xie, C.; Wang, J.; Zhou, T.; Zhou, C.; Li, J.; Bai, J.; Zhu, X.; Zhou, B. Facile, Controllable and Ultrathin NiFe-LDH In Situ Grown on a Ni Foam by Ultrasonic Self-Etching for Highly Efficient Urine Conversion. *Environ. Sci. Technol.* **2023**, *57*, 2939–2948. https://doi.org/10.1021/acs.est.2c07282.
80. Cai, M.; Zhu, Q.; Wang, X.; Shao, Z.; Yao, L.; Zeng, H.; Wu, X.; Chen, J.; Huang, K.; Feng, S. Formation and Stabilization of NiOOH by Introducing α-FeOOH in LDH: Composite Electrocatalyst for Oxygen Evolution and Urea Oxidation Reactions. *Adv. Mater.* **2023**, *35*, 2209338. https://doi.org/10.1002/adma.202209338.
81. Liao, Y.; Chen, Y.; Li, L.; Luo, S.; Qing, Y.; Tian, C.; Xu, H.; Zhang, J.; Wu, Y. Ultrafine Homologous Ni_2P–Co_2P Heterostructures via Space-Confined Topological Transformation for Superior Urea Electrolysis. *Adv. Funct. Mater.* **2023**, *33*, 2303300. https://doi.org/10.1002/adfm.202303300.
82. Zubair, M.; Usov, P.M.; Ohtsu, H.; Yuwono, J.A.; Gerke, C.S.; Foley, G.D.Y.; Hackbarth, H.; Webster, R.F.; Yang, Y.; Lie, W.H.; et al. Vacancy Mediated Electrooxidation of 5-Hydroxymethyl Furfuryl Using Defect Engineered Layered Double Hydroxide Electrocatalysts. *Adv. Energy Mater.* **2024**, *14*, 2400676. https://doi.org/10.1002/aenm.202400676.
83. Yu, H.; Zhu, S.; Hao, Y.; Chang, Y.M.; Li, L.; Ma, J.; Chen, H.Y.; Shao, M.; Peng, S. Modulating Local Interfacial Bonding Environment of Heterostructures for Energy-Saving Hydrogen Production at High Current Densities. *Adv. Funct. Mater.* **2023**, *33*, 2212811. https://doi.org/10.1002/adfm.202212811.
84. Wang, T.; Wang, P.; Zang, W.; Li, X.; Chen, D.; Kou, Z.; Mu, S.; Wang, J. Nanoframes of Co_3O_4–Mo_2N Heterointerfaces Enable High-Performance Bifunctionality toward Both Electrocatalytic HER and OER. *Adv. Funct. Mater.* **2021**, *32*, 2107382. https://doi.org/10.1002/adfm.202107382.
85. Wang, Y.; Chen, D.; Zhang, J.; Balogun, M.S.; Wang, P.; Tong, Y.; Huang, Y. Charge Relays via Dual Carbon-Actions on Nanostructured $BiVO_4$ for High Performance Photoelectrochemical Water Splitting. *Adv. Funct. Mater.* **2022**, *32*, 2112738. https://doi.org/10.1002/adfm.202112738.
86. Gao, X.; Li, X.; Yu, Y.; Kou, Z.; Wang, P.; Liu, X.; Zhang, J.; He, J.; Mu, S.; Wang, J. Synergizing aliovalent doping and interface in heterostructured NiV nitride@oxyhydroxide core-shell nanosheet arrays enables efficient oxygen evolution. *Nano Energy* **2021**, *85*, 105961. https://doi.org/10.1016/j.nanoen.2021.105961.
87. Pei, Y.; Li, D.; Qiu, C.; Yan, L.; Li, Z.; Yu, Z.; Fang, W.; Lu, Y.; Zhang, B. High-Entropy Sulfide Catalyst Boosts Energy-Saving Electrochemical Sulfion Upgrading to Thiosulfate Coupled with Hydrogen Production. *Angew. Chem. Int. Ed.* **2024**, *63*, e202411977. https://doi.org/10.1002/anie.202411977.